

Efficient Unimolecular Deprotonation of Aniline Radical Cations

Gary W. Dombrowski and Joseph P. Dinnocenzo*

Department of Chemistry, University of Rochester, Rochester, New York 14627-0216

Paul A. Zielinski and Samir Farid*

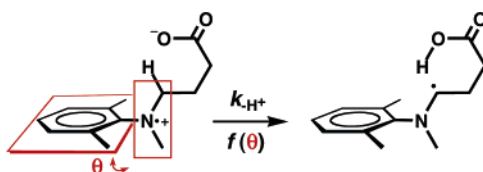
Eastman Kodak Company, Research Laboratories, Rochester, New York 14650-2109

Zofia M. Wosinska and Ian R. Gould*

Department of Chemistry and Biochemistry, Arizona State University, Tempe, Arizona 85287-1604

igould@asu.edu

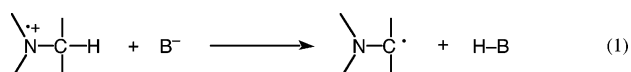
Received December 14, 2004



Deprotonation of the radical cations of aromatic amines, such as anilines, generally occurs much more slowly than other fragmentation reactions. Here we report a stereoelectronic effect involving twisting of the anilino group out of the plane of the benzene ring that results in a significantly increased rate of reactivity toward deprotonation. Quantitative studies of the rate constants for deprotonation as a function of aniline radical cation pK_a (Brønsted plots) demonstrate that the effect is not simply due to a change in the reaction thermodynamics. By combining this stereoelectronic effect with covalent attachment of carboxylate as a base, aniline radical cations that undergo unimolecular deprotonation with rate constants as high as 10^8 s^{-1} , even in unfavorable protic media, are described.

I. Introduction

Deprotonation reactions of amine radical cations to form α -amino radicals have attracted considerable attention because of interest in their mechanisms,¹ and because of their potential synthetic utility.² This simplest fragmentation reaction of a radical cation is illustrated in eq 1 for a generic amine radical cation that undergoes deprotonation by a base, B^- . The α -amino radical product of deprotonation is a very strong reducing agent, which



has added to the interest in amine radical cation fragmentation reactions.³

Deprotonation of amine radical cations is also important in several practical applications of photoinduced electron-transfer reactions.⁴ One recent example in silver halide photography that capitalizes on the strong reduc-

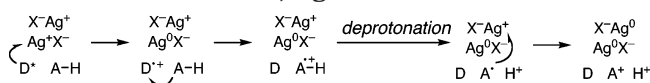
(1) See, for example: (a) Cohen, S. G.; Parola, A.; Parsons, G. H. *Chem. Rev.* **1973**, *73*, 141. (b) Lewis, F. D.; Ho, T.-I.; Simpson, J. T. *J. Org. Chem.* **1981**, *46*, 1077. (c) Lewis, F. D.; Ho, T.-I.; Simpson, J. T. *J. Am. Chem. Soc.* **1982**, *104*, 1924. (d) Davidson, R. S. *Adv. Phys. Org. Chem.* **1983**, *19*, 1. (e) Lewis, F. D. *Acc. Chem. Res.* **1986**, *19*, 401. (f) Nelsen, S. F.; Ippoliti, J. T. *J. Am. Chem. Soc.* **1986**, *108*, 4879. (g) Kavarnos, G. J.; Turro, N. J. *Chem. Rev.* **1986**, *86*, 401. (h) Ci, X.; Silveira da Silva, R.; Nicodem, D.; Whitten, D. G. *J. Am. Chem. Soc.* **1989**, *111*, 1337. (i) Pienta, N. J. *Photoinduced Electron Transfer*; Fox, M. A., Chanon, M., Eds.; Elsevier: New York, 1988; Part C. (j) Kellett, M. A.; Whitten, D. G.; Gould, I. R.; Bergmark, W. R. *J. Am. Chem. Soc.* **1991**, *113*, 358. (k) Dinnocenzo, J. P.; Karki, S. B.; Jones, J. P. *J. Am. Chem. Soc.* **1993**, *115*, 7111. (l) Yoon, U. C.; Mariano, P. S.; Givens, R. S.; Atwater, B. W. *Adv. Electron Transfer* **1994**, *4*, 117. (m) Yoon, U. C.; Mariano, P. S. *J. Photosci.* **2003**, *10*, 89.

(2) (a) Mariano, P. S.; Stavinola, J. L. In *Synthetic Organic Photochemistry*; Horspool, W. M., Ed.; Plenum Press: New York, 1984; Chapter 3. (b) Jeon, Y. T.; Lee, C. P.; Mariano, P. S. *J. Am. Chem. Soc.* **1991**, *113*, 8863. (c) Xu, W.; Mariano, P. S. *J. Am. Chem. Soc.* **1991**, *113*, 1431. (d) Yoon, U. C.; Mariano, P. S. *Acc. Chem. Res.* **1992**, *25*, 233. (e) Yoon, U. C.; Mariano, P. S. *Acc. Chem. Res.* **2001**, *34*, 523.

(3) (a) Wayner, D. D. M.; Dannenberg, J. J.; Griller, D. *Chem. Phys. Lett.* **1986**, *131*, 189. (b) Wayner, D. D. M.; McPhee, D. J.; Griller, D. *J. Am. Chem. Soc.* **1988**, *110*, 132. (c) Jockusch, S.; Timpe, H.-J.; Schnabel, W.; Turro, N. J. *J. Photochem. Photobiol. A: Chem.* **1996**, *96*, 129.

(4) (a) Reiser, A. *Photoreactive Polymers, the Science and Technology of Resists*; Wiley: New York, 1989. (b) Paczkowski, J.; Neckers, D. C. In *Electron Transfer in Chemistry*; Balzani, V., Ed.; Wiley-VCH: New York, 2001; Vol. 5, p 516.

SCHEME 1. Schematic Illustration of the Two-Electron-Sensitization Scheme, Showing Injection of Two Electrons into the Conduction Band of Silver Halide, Ag^+X^- ^a

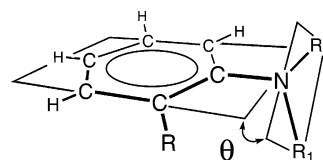


^a The trapped electrons are indicated as Ag^0 .

ing power of the α -amino radical is two-electron sensitization.⁵ Here, light absorption to form the excited state of a photographic sensitizing dye, D^* , which is adsorbed on the surface of microcrystalline silver halide, Ag^+X^- , results in transfer of an electron into the conduction band and formation of the dye radical cation, D^+ , Scheme 1. In the presence of an appropriate amine additive, A-H , donation of an electron to D^+ can occur to form the amine radical cation, A-H^+ . Fragmentation (in this case deprotonation) of A-H^+ forms an α -amino radical, A^* , that injects a second electron into the conduction band, Scheme 1. Thus, two electrons can be transferred per absorbed photon, thereby doubling the photographic response.⁵

Decarboxylation and desilylation fragmentation reactions of amine radical cations have been successfully implemented in two-electron sensitization schemes;⁶ however, the corresponding deprotonation reaction initially posed a challenge. Alkylamines, whose radical cations have been shown to undergo relatively facile deprotonation,⁷ cannot be used in aqueous photographic emulsions because they would be protonated and thus not function as electron donors. In addition, Mariano et al. have clearly shown that deprotonation of aromatic amine radical cations tends to be much slower than other possible fragmentation reactions, and is thus often less useful.⁸ The kinetics of deprotonation, as well as other fragmentation reactions of the radical cations, are expected to increase with increasing oxidation potential of the amine.⁹ This is not a generally useful solution to the problem of low kinetic reactivity, especially in the two-electron sensitization application, since increasing the oxidation potential reduces the ability of the amine to act as an electron donor. Thus, an alternate method was required for controlling the reactivity of amine radical cations. We have found a stereoelectronic effect that can significantly increase the rate constants for deprotonation of aniline radical cations.¹⁰ Based upon this effect, aniline derivatives have been designed with a covalently at-

SCHEME 2. The Angle θ Is the Dihedral Angle between the Plane Containing the Benzene Ring and That Containing the Nitrogen and the Carbons of the α -Methyl Groups



tached base that undergo efficient *unimolecular* (intramolecular) deprotonation upon one-electron oxidation. Here we describe anilines that have relatively low oxidation potentials, and whose radical cations deprotonate with controllable rate constants over 4 orders of magnitude. Reactions with rate constants approaching 10^8 s^{-1} have been obtained, even in unfavorable protic media.

The first part of this paper describes kinetic and thermodynamic studies of the rate constants for bimolecular deprotonation of aromatic amine radical cations that delineate the stereoelectronic effect. The second part describes structures that undergo unimolecular fragmentation. The paper concludes with a discussion of other factors that control the deprotonation reactions of amine radical cations.

II. Results and Discussion

II. A. Bimolecular Deprotonation. Anilines in which ortho substituents (R , Scheme 2) twist the nitrogen out of conjugation with the benzene ring are known to be more basic than simple anilines.¹¹ This is understood as a consequence of localization of the nonbonding electrons on nitrogen, which increases their basicity. It seemed reasonable that similar twisting might also help to localize the spin and positive charge close to the nitrogen in the corresponding radical cations, thus enhancing the electrophilicity of hydrogen atoms on carbons α to the nitrogen. The kinetics of amine radical cation deprotonation have been studied previously with a variety of techniques.^{8,12} Rate constants are expected to depend on the thermodynamics of the reaction, i.e., on the strength of the base and the $\text{p}K_a$ of the radical cation, and this has been shown to be the case for several amines, and other radical cations.^{8a,13,14} Indeed, two previous studies have specifically addressed the relationship between kinetics and thermodynamics of deprotonation of sub-

(10) Deprotonation would also be expected to be faster with increasing stability of the radical product, and this has also been confirmed experimentally.^{8a}

(11) Ingold, C. K. *Structure and Mechanism in Organic Chemistry*; Cornell University Press: Ithaca, NY, 1953; Chapter XIII.

(12) (a) Powell, M. F.; Wu, J. C.; Bruce, T. C. *J. Am. Chem. Soc.* **1984**, *106*, 3850. (b) Sinha, A.; Bruce, T. C. *J. Am. Chem. Soc.* **1984**, *106*, 7291. (c) Fukuzumi, S.; Kondo, Y.; Tanaka, T. *J. Chem. Soc., Perkin Trans. 2* **1984**, 673. (d) Das, S.; Von Sonntag, C. *Z. Naturforsch.* **1986**, *416*, 505. (e) Hapiot, P.; Moiroux, J.; Saveant, J.-M. *J. Am. Chem. Soc.* **1990**, *112*, 1337. (f) Anne, A.; Hapiot, P.; Moiroux, J.; Neta, P.; Saveant, J.-M. *J. Phys. Chem.* **1991**, *95*, 2370. (g) Fukuzumi, S.; Tokuda, Y.; Kitano, T.; Okamoto, T.; Otera, J. *J. Am. Chem. Soc.* **1993**, *115*, 8960. (h) Anne, A.; Fraoua, S.; Hapiot, P.; Moiroux, J.; Saveant, J.-M. *J. Am. Chem. Soc.* **1995**, *117*, 7412. (i) Goez, M.; Sartorius, I. *J. Phys. Chem. A* **2003**, *107*, 8539.

(13) (a) Dinnocenzo, J. P.; Banach, T. E. *J. Am. Chem. Soc.* **1989**, *111*, 8646. (b) Parker, V. D.; Tilst, M. *J. Am. Chem. Soc.* **1991**, *113*, 8778. (c) Agnes, A.; Hapiot, P.; Moiroux, J.; Neta, P.; Saveant, J.-M. *J. Am. Chem. Soc.* **1992**, *114*, 4694.

(5) (a) Gould, I. R.; Lenhard, J. R.; Muentner, A. A.; Godleski, S. A.; Farid, S. *J. Am. Chem. Soc.* **2000**, *122*, 11934. (b) Gould, I. R.; Lenhard, J. R.; Muentner, A. A.; Godleski, S. A.; Farid, S. *Pure Appl. Chem.* **2001**, *73*, 455.

(6) (a) Gould, I. R.; Godleski, S. A.; Zielinski, P. A.; Farid, S. *Can. J. Chem.* **2003**, *81*, 777. (b) Gould, I. R.; Farid, S. *J. Phys. Chem. A* **2004**, *108*, 10949.

(7) See, for example: Davidson, R. S. *Adv. Phys. Org. Chem.* **1983**, *19*, 1.

(8) (a) Zhang, X.; Yeh, S.-R.; Hong, S.; Freccero, M.; Albin, A.; Falvey, D. E.; Mariano, P. S. *J. Am. Chem. Soc.* **1994**, *116*, 4211. (b) Su, Z.; Falvey, D. E.; Yoon, U. C.; Mariano, P. S. *J. Am. Chem. Soc.* **1997**, *119*, 5261. (c) Su, Z.; Mariano, P. S.; Falvey, D. E.; Yoon, U. C.; Oh, S. W. *J. Am. Chem. Soc.* **1998**, *120*, 10676. (d) Yoon, U. C.; Kwon, H. C.; Hyung, T. G.; Choi, K. H.; Oh, S. W.; Yang, S.; Zhao, Z.; Mariano, P. S. *J. Am. Chem. Soc.* **2004**, *126*, 1110.

(9) (a) Nicholas, A. M. P.; Arnold, D. R. *Can. J. Chem.* **1982**, *60*, 2165. (b) Arnold, D. R.; Snow, M. S. *Can. J. Chem.* **1985**, *66*, 3012. (c) Gaillard, E. R.; Whitten, D. G. *Acc. Chem. Res.* **1996**, *29*, 292.

TABLE 1. Spectral, Kinetic, and Thermodynamic Properties Related to Deprotonation of Aromatic Amine Radical Cations with Tetrabutylammonium Acetate as the Base in Acetonitrile Containing 0.5 M Water and 0.5 M Tetrabutylammonium Perchlorate

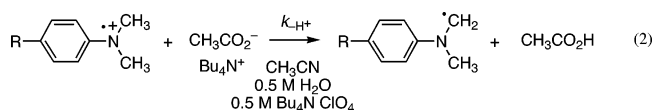
Structure	Compound	λ_{max}^a (nm)	$k_{\text{H}^+}^b$ ($\text{M}^{-1} \text{s}^{-1}$)	$k_{\text{H}^+}/k_{\text{D}^+}^c$	$E^{\text{ox}d}$ (V vs SCE)	BDE e (kcal mol $^{-1}$)	$\text{p}K_{\text{a}}^{*f}$
	1a	490	1.1×10^7	--	0.55	91 g	23.2
	1b	470	4.1×10^7	1.6	0.72	89.8	19.5
	1c	470	1.2×10^8	2.1	0.84	91.7	18.8
	1d	-- h	1.7×10^8	2.4	0.89	89.8	16.6
	1e	470	1.4×10^9	1.7	1.11	92.2	14.6
	2	470	2.4×10^8	--	0.90	91 g	17.3
	3	520 i	4.9×10^9	2.4	1.12	94.7	16.3
	4	530	3.6×10^9	--	0.94	90.2	16.0

a Absorption maximum of the radical cation in the visible region.

b Rate constant for deprotonation at room temperature. c Obtained by comparing $\text{ArN}(\text{CH}_3)_2$ to $\text{ArN}(\text{CD}_3)_2$. d Oxidation potentials measured as described in the Experimental Section. e Data taken from ref 15, unless otherwise indicated. f Calculated with eq 3. g Not measured, value taken as the average of the measured values for related compounds. h Not measured, kinetics determined at 470 nm. i The absorption maximum for this radical cation varied somewhat with time. 20b

stituted dimethylaniline radical cations. 8a,13b However, the deprotonation rate constants are found to depend strongly upon reaction conditions. 8a To clearly delineate the stereoelectronic effect, we revisited the kinetics of these deprotonation reactions using a quantitative Brønsted analysis that allowed comparison of the twisted and nontwisted anilines under *identical* conditions. The $\text{p}K_{\text{a}}$ values for the radical cations have also been recalculated by using our recently revised $\alpha\text{-C-H}$ bond dissociation energies for the *N,N*-dimethylanilines. 15

Bimolecular rate constants, k_{H^+} , for deprotonation of the radical cations of the 4-substituted *N,N*-dimethylanilines **1a–e**, Table 1, were determined in acetonitrile solution at room temperature, using tetrabutylammonium acetate as the external base, eq 2. The radical



cations were generated in time-resolved experiments by using cyanoanthracene/cosensitization, 16 as described in detail elsewhere for studies of related aniline radical

(14) (a) Schlesener, C. J.; Amatore, C.; Kochi, J. K. *J. Am. Chem. Soc.* **1984**, *106*, 3567. (b) Schlesener, C. J.; Amatore, C.; Kochi, J. K. *J. Am. Chem. Soc.* **1984**, *106*, 7472. (c) Schlesener, C. J.; Amatore, C.; Kochi, J. K. *J. Phys. Chem.* **1986**, *90*, 3747. (d) Anne, A.; Fraoua, S.; Grass, V.; Moiroux, J.; Saveant, J.-M. *J. Am. Chem. Soc.* **1988**, *110*, 2951.

(15) Dombrowski, G. W.; Dinnocenzo, J. P.; Farid, S.; Goodman, J. L.; Gould, I. R. *J. Org. Chem.* **1999**, *64*, 427.

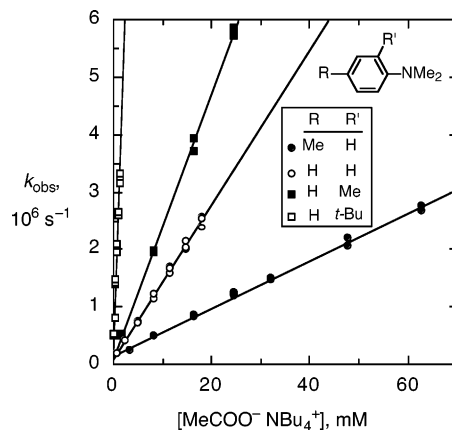


FIGURE 1. Plots of observed rate of pseudo-first-order decay, k_{obs} , versus concentration of tetrabutylammonium acetate for deprotonation of the radical cations of (open circles) *N,N*-dimethylaniline, **1c**, and *N,N*-dimethylaniline with a 4-methyl substituent, **1b**, (filled squares) a 2-methyl substituent, **2**, and (open squares) a 2-*tert*-butyl substituent, **3**, in acetonitrile with 0.5 M water and 0.5 M tetramethylammonium perchlorate, at room temperature.

cations. 6,17 The deprotonation rate constants were determined from the slopes of plots of the observed pseudo-first-order decay rate constants of the radical cations monitored at their absorption maxima, k_{obs} , as a function of the concentration of added acetate ion. The basicity of the acetate anion is expected to be strongly dependent upon adventitious water, and therefore to ensure reproducibility in the measured rate constants the reactions were performed in the presence of 0.5 M water. To eliminate the effect of changing ionic strength with increasing acetate concentration, the reactions were also performed in the presence of 0.5 M tetrabutylammonium perchlorate. Further details are given in the Experimental Section. Typical data are given in Figure 1 and the rate constants are summarized in Table 1.

The observed bimolecular reactions between the radical cations and the acetate were assigned to deprotonation based on the similarity of the results to those previously described, 8a on the response of the reaction rate constants to changes in structure of the anilines, and also on the basis of observed primary deuterium isotope effects discussed below.

Relating the kinetics and thermodynamics of the deprotonation reactions requires determination of the $\text{p}K_{\text{a}}$ of the radical cations. 9 The usual approach uses a thermodynamic cycle, as shown in Scheme 3, and eq 3a to determine the C–H bond dissociation energies of the radical cations, BDE^{*+} . 13a The corresponding $\text{p}K_{\text{a}}^{*+}$ values for the radical cations are obtained from the BDE^{*+} according to eq 3b. The relevant data are collected in Table 1.

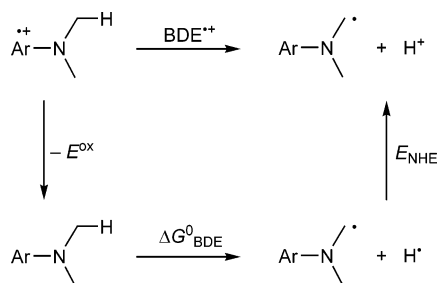
$$\text{BDE}^{*+} = \Delta G_{\text{BDE}}^{\circ} + E_{\text{NHE}} + E^{\text{ox}} \quad (3a)$$

$$\text{p}K_{\text{a}}^{*+} = \text{BDE}^{*+}/2.303 RT \quad (3b)$$

(16) Gould, I. R.; Ege, D.; Moser, J. E.; Farid, S. *J. Am. Chem. Soc.* **1990**, *112*, 4290.

(17) Experimental details are given in ref 5a.

SCHEME 3



From the data in Table 1 it is clear that, as previously observed, increasing the pK_a^{+} of the aniline radical cation results in a corresponding decrease in the rate constant for deprotonation.^{8a,13b} This effect is illustrated graphically in Figure 2, which shows a Brønsted plot of $\log(k_{-H^+})$ versus pK_a^{+} for these reactions.

These data are in general agreement with several other quantitative studies of deprotonation of amine radical cations.^{8a,13b} The difference in the rate constants for the slowest (**1a**) and the fastest (**1e**) of the 4-substituted anilines measured in this work is ca. 2 orders of magnitude. It is interesting that Mariano et al. obtained a very similar relative rate difference for these same two reactions,^{8a} although their absolute rate constants are roughly 2 orders of magnitude smaller than those reported here. Presumably, this is because the solvent mixture used by Mariano et al. was more “protic” (i.e. 60:40 methanol:acetonitrile) than that used in the present experiments (0.5 M water in acetonitrile corresponds to ca. 1% water in acetonitrile), which should reduce the basicity of the carboxylate.¹⁸

Included in Table 1 are rate constants for reaction of acetate anion with several of the aniline radical cations, where the hydrogens on the *N*-methyl groups have been deuterated. Primary isotope effects were found, consistent with C–H bond breaking in the transition state, i.e., deprotonation. Mariano et al. observed a somewhat larger isotope effect for deprotonation of the unsubstituted *N,N*-dimethylaniline radical cation **1c**.^{8a} The relatively small kinetic isotope effects are also consistent with a fairly early transition state,¹⁹ and of course this is quite reasonable given the large absolute values of the rate constants, Table 1. Consistent with this conclusion is the slope of the Brønsted plot for the 4-substituted anilines of -0.23 . Such a small slope would normally be associated with a small extent of proton transfer in the transition state.¹⁹

The Brønsted plot is quite linear over 2 orders of magnitude in rate constant. Previously, Saveant et al. analyzed the rate constants for deprotonation of a series of NADH derivatives using a Marcus-type analysis, i.e., a nonlinear free energy relationship.^{13c} In the present case, however, since the data fit reasonably well to a linear relationship, there is obviously no additional information that can be obtained from a nonlinear fit.

The radical cations of several dimethylanilines with substituents in the ortho positions were examined by using B3LPY/6-31G* computations. The structures of

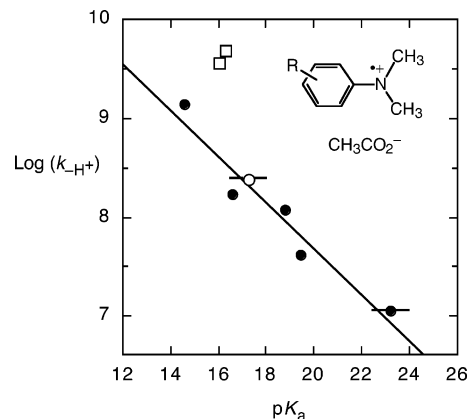
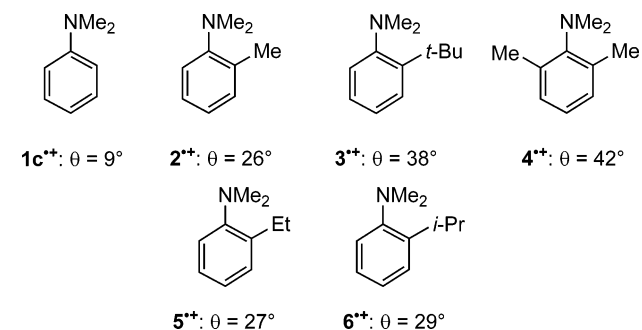


FIGURE 2. Brønsted plot of the logarithm of the bimolecular rate constant for deprotonation of the radical cations of *N,N*-dimethylaniline derivatives: (closed circles) 4-substituted-*N,N*-dimethylanilines, **1a–1e**; (open circle) *N,N*,2-trimethylaniline, **2**; (open squares) 2-*tert*-butyl-*N,N*-dimethylaniline, **3**; and *N,N*,2,6-tetramethylaniline, **4**. The straight line represents the best fit to the 4-substituted anilines and is characterized by a slope of -0.23 and intercept of 12.3.

SCHEME 4. Structures of Sterically Twisted *N,N*-Dimethylaniline Radical Cations, and the Dihedral Angles between the Planes Containing the Aromatic Ring and the Amino Nitrogen, θ , As Defined in Scheme 2



these compounds, **2–6**, are summarized in Scheme 4, together with the dihedral angles between the plane containing the aromatic ring and that containing the nitrogen, θ (hereafter referred to as the twist angle), as defined in Scheme 2. Also given is the corresponding angle for the parent dimethylaniline radical cation, **1c**⁺. Not surprisingly, the twist angle increases with increasing bulk of the ortho substituent, with the *N,N*,2,6-tetramethylaniline radical cation, **4**⁺, being the most twisted.

The radical cations of three of these, **2**⁺–**4**⁺, were also studied experimentally under the same conditions as for the para-substituted anilines. As illustrated in Figure 3, the transient absorption spectrum of the radical cation of **2** is virtually identical with that of the parent *N,N*-dimethylaniline **1c**. The more highly twisted **3**⁺ and **4**⁺, however, give radical cations with increasingly broadened spectra and red-shifted absorption maxima.²⁰

(20) (a) In addition to red-shifting, the extinction coefficient at the absorption maxima also decrease with increased twisting, although accurate measurements of this effect were not made. (b) The absorption spectrum of **3**⁺ exhibited a slight red-shift over a 1–2 μ s time scale under the experimental conditions; see Supporting Information, Figure S3.

(18) Isaacs, N. *Physical Organic Chemistry*; Longman: Harlow, England, 1987.

(19) Ritchie, C. D. *Physical Organic Chemistry. The Fundamental Concepts*; Marcel Dekker: New York, 1975.

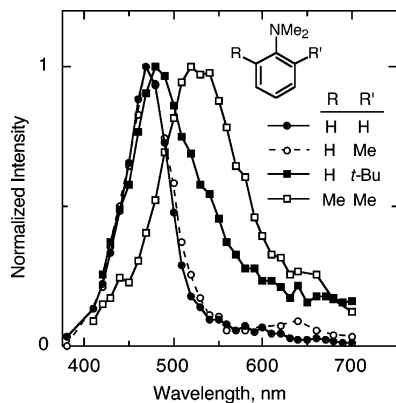
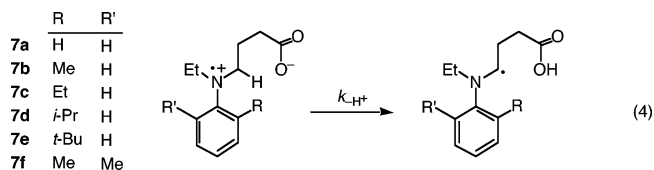


FIGURE 3. Absorption spectra of the radical cations of (closed circles) *N,N*-dimethylaniline, **1c**, and *N,N*-dimethylaniline with (open circles) a 2-methyl substituent, **2**, (closed squares) a 2-*tert*-butyl substituent, **3**, and (open squares) 2,6-dimethyl substituents, **4**, in acetonitrile containing 0.5 M water and 0.5 M tetrabutylammonium perchlorate, at room temperature.²⁰

Rate constants for deprotonation of the radical cations of **2–4** were measured under the same conditions used for compounds **1a–1e**, Table 1. Compared to the unsubstituted aniline **1c**⁺, the reactivity increases roughly with increasing twist of the dimethylamino group, with deprotonation of the more highly twisted **3**⁺ and **4**⁺ being ca. 30 times faster than that of the parent aniline **1c**⁺.

Twisting the aryl group results in an increase in the oxidation potential of the amines compared to that of the parent *N,N*-dimethylaniline **1c**, Table 1. Thus, deprotonations of **2**⁺–**4**⁺ are more exothermic than **1c**⁺. However, the Brønsted plot of Figure 2 shows that, whereas the influence on the rate constant is hardly noticeable for the less twisted derivative, **2**⁺, the rate constants for the strongly twisted **3**⁺ and **4**⁺ are approximately an order of magnitude larger than would have been predicted from the 4-substituted aniline data. This clearly indicates that the rate increase is not simply due to an increase in the driving force for these reactions, but is a true stereoelectronic effect. Indeed, the rate constants for deprotonation of **3**⁺ and **4**⁺ are sufficiently high that they are close to the diffusion-controlled limit (ca. $4 \times 10^9 \text{ M}^{-1} \text{ s}^{-1}$), which suggests that an order of magnitude probably represents a lower limit to the increase in the rate constant as a result of charge localization.

II. B. Intramolecular Deprotonation of Twisted Anilines. The utility of a deprotonation reaction that does not require an external base is obvious. We have investigated the reactivity of aniline radical cations in which a carboxylate functional group is included as a substituent, structures **7**, eq 4. The clear result from the



bimolecular reactions is that deprotonation is faster when delocalization of the charge is minimized, thus we expected that the rate of intramolecular deprotonation should increase with increasing twist angle in structures **7**. The carboxylate is attached to the nitrogen via a three-

TABLE 2. Kinetic Parameters for Intramolecular Deprotonation of the Radical Cations of Aniline Derivatives, **7a–f**, with Varying Substituents in the Ortho Position, Measured in Acetonitrile with 20% Water

R	R'	compd	k_{-H^+} (s^{-1})	E_a^a (kcal/mol)	$\log(A)^a$ (s^{-1})
H	H	7a	$<5 \times 10^4$ ^b (5×10^5) ^c	^b	^b (14.3) ^c
Me	H	7b	2.0×10^5	12.9	14.9
Et	H	7c	5.9×10^5	12.6	15.1
<i>i</i> -Pr	H	7d	1.8×10^6	11.6	14.8
<i>t</i> -Bu	H	7e	$\sim 4 \times 10^7$ ^d		
Me	Me	7f	$\sim 9 \times 10^7$ ^d		

^a Arrhenius activation energy, E_a , and intercept of Arrhenius plot, $\log(A)$. ^b This reaction under these conditions was too slow to be measured.²¹ ^c Data for acetonitrile with 0.5 M water. ^d Estimated value, see text.

carbon chain, since this both prevents decarboxylation in the radical cation^{6b,8a} and also allows a six-membered ring in the transition state for deprotonation, as discussed further below.

II. B. i. Reaction Kinetics. These reactions were studied in acetonitrile with a higher water content than used in the bimolecular studies for two reasons. First, the observed rates of decay of the radical cations in the unimolecular reactions were found to be significantly larger than those of the pseudo-first-order rate constants in the bimolecular reactions at the external base concentrations used. The use of 20% water, compared to the 0.5 M (ca. 1%) water used in the bimolecular reactions, decreases the rate of reaction into a range that can be readily determined by using our time-resolved apparatus. Second, the kinetics of the unimolecular deprotonation reactions could be directly compared to corresponding decarboxylation and desilylation reactions for two-electron sensitization application, since these were also studied in 20% aqueous acetonitrile.^{6,17}

In the solvent mixture 20% water in acetonitrile, the radical cations of the anilines **7a–f** exhibited transient absorption spectra that were similar to those of the corresponding *N,N*-dimethylanilines given in Figure 3 (data not shown). The time-resolved decays of the radical cation absorptions were observed to be first order, and were assigned to intramolecular deprotonation on the basis of the fact that the decay rates responded to molecular structure in a manner consistent with this reaction (see below). In addition, the α -amino radical, the product of deprotonation, eq 4, was shown to transfer an electron to 9,10-dicyanoanthracene, as described elsewhere for related systems.¹⁷ Finally, at the concentrations of the anilines used in the experiments (ca. 2–4 mM), the rates of intermolecular deprotonation were much slower than the corresponding rates of intramolecular deprotonation (see also below).

Table 2 summarizes the rate constants for unimolecular deprotonation in the radical cations of **7a–f**. With increasing twist angle, the rate constant increases by more than 3 orders of magnitude: from $<5 \times 10^4$ for the

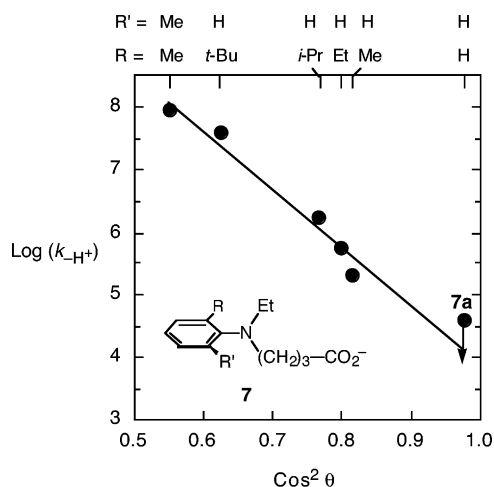


FIGURE 4. Plot of the logarithm of the rate constant for unimolecular deprotonation ($\log(k_{-H^+})$) versus the cosine squared of the dihedral angle θ , defined in Scheme 1, for the simple dimethylanilines, assumed to be appropriate for the intramolecular deprotonating anilines here. The point for the radical cation of **7a** (indicated) is a maximum value.²¹

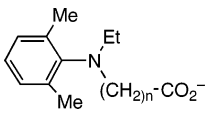
unsubstituted compound **7a** to $\sim 9 \times 10^7 \text{ s}^{-1}$ for the *o,o'*-dimethyl compound **7f**.²¹

The combined stereoelectronic effect and increase in oxidation potential with increasing twisting in the unimolecular systems is quite dramatic. The extent of charge delocalization is likely to be related to the extent of orbital overlap of the aromatic π system and the nonbonding orbital on nitrogen. In turn, this can be related to $\cos^2\theta$, where θ is the twist angle. A plot of $\log(k_{-H^+})$ versus $\cos^2\theta$, where the values of θ are assumed to be the same as those for the corresponding simple dimethylanilines from Scheme 4, is shown in Figure 4. This plot is remarkably linear, even though there is no reason to expect a strictly linear relationship, and clearly indicates how twisting can be used to control the rate of deprotonation over nearly 4 orders of magnitude.

II. B. ii. Effect of Tether Length. Another way in which the rate constant for unimolecular deprotonation could in principle be controlled is by varying the length of the methylene chain, $(\text{CH}_2)_n$, between the carboxylate group and the nitrogen. The shortest tether is $-(\text{CH}_2)_2-$, because the radical cations of derivatives with one methylene unit are likely to undergo decarboxylation rather than deprotonation.^{6b,5c} In addition to **7f**, we investigated the deprotonation of the radical cations of other derivatives, compounds **7g–j**, Table 3, in which the two *o*-methyl groups enhanced charge localization around the nitrogen, and where the number of methylene groups, n , was varied from 2 to 6. The results are summarized in Table 3.

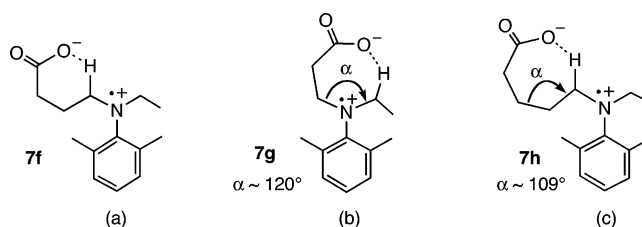
(21) For compound **7a**, intramolecular deprotonation in acetonitrile with 20% water was too slow to measure, because of the combined low kinetic acidity of this untwisted amine radical cation moiety, and the low kinetic basicity of the carboxylate under these conditions. The observed rate of decay at room temperature was $5 \times 10^4 \text{ s}^{-1}$; however, the reaction had Arrhenius activation parameters that were very different from the other reactions, i.e., $E_a = 3.8 \text{ kcal/mol}$ and $\log(A) = 7.7$. These parameters would be more consistent with a bimolecular reaction, for example, quenching by impurities. The activation parameters with 0.5 M water, where the carboxylate basicity is much larger, Table 2, are consistent with deprotonation under these conditions. Thus, we assign the observed rate of $5 \times 10^4 \text{ s}^{-1}$ in 20% water to be the *maximum* rate constant for unimolecular deprotonation.

TABLE 3. Rate Constants and Activation Parameters for Intramolecular Deprotonation of Aniline Radical Cations as a Function of the Length of the Methylene Chain Connecting the Nitrogen Atom to the Carboxylate Group, Measured in Acetonitrile with 20% Water

compd	k_{-H^+} (s^{-1})	E_a^a (kcal/mol)	$\log(A)^a$ (s^{-1})
	7g	1.8×10^6	12.4
$n = 2$	7f	$\sim 9 \times 10^7$ ^b	15.4
$n = 3$	7h	1.3×10^7	14.6
$n = 4$	7i	1.4×10^6	14.3
$n = 5$	7j	2.3×10^5	13.7
$n = 6$			

^a Arrhenius activation energy, E_a , and intercept of Arrhenius plot, $\log(A)$. ^b Estimated value, see text.

SCHEME 5



Not surprisingly, the maximum rate constant is attained for **7f**, with $n = 3$, which has a six-membered ring transition state for radical cation deprotonation, Scheme 5a. With each additional methylene group in the chain, the rate constant decreases by an average factor of ~ 7 – 8 , Figure 5. It is noteworthy that with $n = 2$ (compound **7g**), which has a five-membered ring transition state for deprotonation from the chain containing the carboxylate, proton transfer from the α -carbon of the ethyl group would have a seven-membered-ring transition state, Scheme 5b. The rate constant for **7g**, however, is lower, by a factor of ~ 7 , compared to that for **7h**, which reacts through a seven-membered transition state for deprotonation on the same chain as the carboxylate, Scheme 5c.²² An unfavorable conformation for the intrachain reaction in **7g**, relative to that for interchain reaction in **7h**, is likely to be the reason for the different reactivities of these two seven-membered-ring transition state reactions. The most favorable transition state will presumably be favored by two structural features: (1) a linear or near-linear O–H–C bond angle and (2) a collinear or near-collinear alignment of the C–H bond and the p-orbital at nitrogen.

Pictorial representations of the transition states for the two reactions are given in Figure 6. These were obtained from a B3LYP/6-31G* optimized structure for *N,N*,2,6-tetramethylaniline, with addition of the appropriate side chains to make **7g** and **7h**. The appropriate torsional angles were adjusted manually to create transition state structures that optimize the structural features cited above (the structures are not optimized in any other way). The structures show that for the “same chain” proton transfer in **7h**, a structure with a O–H–C angle close to

(22) The factor of ~ 7 is, of course, a lower limit for the difference in reactivity between the two seven-membered transition states in compounds **7g** and **7h**, because the intrachain reaction in **7g**, the five-membered-ring transition state, is unlikely to be negligible.

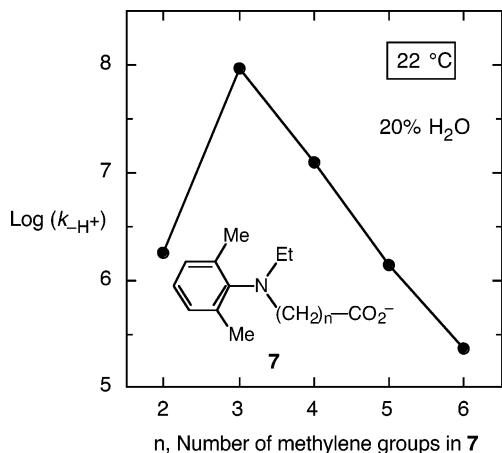


FIGURE 5. Plot of the logarithm of the rate constant for unimolecular deprotonation ($\log(k_{-H^+})$) versus the number of methylenes separating the nitrogen and carboxylate.

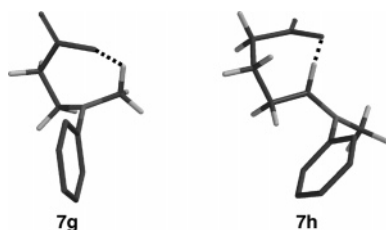


FIGURE 6. Tube models of schematic transition states for the different seven-membered cyclic ring intramolecular deprotonations in the radical cations of **7g** and **7h** (see text for explanation), showing how a collinear arrangement of the O–H–C atoms is impossible in **7g**. For clarity, the hydrogen and methyl substituents have been removed from the benzene rings.

180° is possible (the O, H, and C atoms are close to collinear). In contrast, this is not possible in the transition state for proton transfer from the *N*-ethyl substituent in **7g**.

These structural differences can be understood in a simple way. Shown in Scheme 5, parts b and c, are both seven-membered deprotonation transition states. The key structural difference between the two transition states is the bond angle α , which is ca. 120° and ca. 109° for **7g** and **7h**, respectively. The larger angle for **7g** is a consequence of rehybridization at nitrogen (flattening) upon oxidation. The smaller angle for **7h** allows the carboxylate group to access a more optimal geometry in the transition state.

II. C. Intramolecular Reactions of Nontwisted Anilines. Intramolecular reactivity in a series of substituted anilines without ortho substituents, i.e., nontwisted anilines **8**, Table 4, was also investigated. Intramolecular deprotonation in the radical cations of **8a–d** was significantly slower than that in the radical cations of the corresponding twisted anilines, **7f–j**. Indeed, these reactions could only be studied in solutions with much lower water content and above room temperature. Some kinetic data for these compounds are shown in Figure 7, in acetonitrile solutions with varying water content and at 41 °C, as a function of varying chain length of the methylene tether. The data are summarized in Table 4.

TABLE 4. Rate Constants for Intramolecular Deprotonation of Nontwisted Aniline Radical Cations as a Function of the Length of the Methylene Chain Connecting the Nitrogen Atom to the Carboxylate Group, Measured in Acetonitrile with 1%, 2%, and 4% Water

	compd	k_{-H^+} (s^{-1})		
		1% H ₂ O	2% H ₂ O	4% H ₂ O
$n = 3$	8a	1.3×10^6	4.8×10^5	1.6×10^5
$n = 4$	8b		3.4×10^5	
$n = 5$	8c	6.8×10^5	2.2×10^5	9.3×10^4
$n = 6$	8d	6.5×10^5	2.4×10^5	9.0×10^4

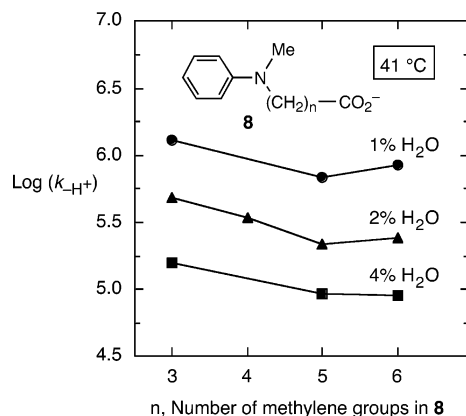


FIGURE 7. Plot of the logarithm of the rate constant for unimolecular deprotonation ($\log(k_{-H^+})$) of the radical cations of ring-unsubstituted aniline derivatives (**8**) with varying length of the methylene chain.

Whereas the rate constant for deprotonation of the twisted, *o,o'*-dimethyl derivative with 3 methylene groups, **7f**, at room temperature and in the presence of 20% water is ca. $10^8 s^{-1}$, that of the corresponding unsubstituted compound **8a** at 41 °C, and in the presence of only 4% water, is ca. $10^5 s^{-1}$. Since the rate constant for deprotonation decreases with increasing water content and with decreasing temperature, the reactivity difference between these two compounds appears to be more than 4 orders of magnitude!

In addition to the much lower rate constants for deprotonation, the radical cations of the nontwisted compounds **8a–d** show very little dependence on the length of the methylene chain. This is in contrast to the corresponding twisted derivatives, **7f–j**, for which the rate constants vary by two and half orders of magnitude between the $(CH_2)_3$ and $(CH_2)_6$ analogues.

For **8a–d**, intramolecular deprotonation of the radical cations was so slow that it could be clearly distinguished from the corresponding intermolecular reaction. Experiments were performed in which the observed decay rate of the radical cations was measured as a function of the concentration of **8** (data not shown), with 1% water at 41 °C. The slopes of these plots gave intermolecular rate constants for the radical cations of **8a–d** of $\sim 9 \pm 2 \times 10^7 M^{-1} s^{-1}$. These can be compared to a bimolecular rate constant of $2.5 \times 10^8 M^{-1} s^{-1}$ determined for deprotonation of the radical cation of *N,N*-dimethylaniline (**1c⁺**) by acetate anion, also measured at 41 °C and under similar reaction conditions (data not shown). The simi-

larity of the rate constants confirms that the carboxylate base and the aniline radical cation parts of $8\mathbf{a}^+ - \mathbf{d}^+$ exhibit normal reactivity in a bimolecular reaction.

The intercepts of the plots of rate versus concentration of $\mathbf{8}$ correspond to the intramolecular rate constants. The ratio of the intercepts to the slopes thus yields the “effective molarities” for the reactions.²³ The values obtained, ca. 0.01 M, are extremely low, since values considerably greater than unity are often found when comparing equivalent inter- and intramolecular reactions.²³ Quite different behavior was observed for the corresponding reactions of the twisted radical cations. Indeed, it was not possible to determine the corresponding effective molarity in these cases since the intramolecular reactions were too fast. For example, the rate constant for intramolecular reaction of $7\mathbf{f}^+$ in 20% aqueous acetonitrile at room temperature is ca. 10^8 s^{-1} (Table 3). The rate constant for the closest corresponding bimolecular reaction, i.e., 4^+ with acetate, is approximately 30 times larger, $3.6 \times 10^9 \text{ M}^{-1} \text{ s}^{-1}$ (Table 1). However, this is in the presence of only 0.9% water. With 20% water, the bimolecular rate constant would probably be much more than 30 times smaller than this (see, for example, Figure S4 in the Supporting Information). Thus, the effective molarities for the radical cations of the twisted anilines are almost certainly much greater than 1 M.

Together, these observations suggest that the rate-determining steps for the inter- and intramolecular reactions may be quite different compared with those in the reactions of the nontwisted anilines. The comparatively small rate constants for the 8^+ suggest that the rate-determining steps are associated with reasonably large activation barriers that do not depend on the ring size of the transition state for deprotonation. The origin of the difference between the chain length dependencies for the twisted and untwisted aniline radical cation deprotonations is unclear. It may involve rotamers associated with the methylene chain that joins the anilino and carboxylate moieties, or the difference may result from different stereoelectronic requirements for the deprotonations.

II. D. Energetic Considerations. Several of the rate constants for both unimolecular and bimolecular deprotonation reactions were measured as a function of temperature. The Arrhenius parameters are summarized in Tables 2 and 3 for the intramolecular reactions of the radical cations of compounds $7\mathbf{a} - \mathbf{f}$, and in Table 5 for the bimolecular reactions of the 4-substituted dimethylanilines $1 - 4$. Typical plots for the bimolecular reactions are included in the Supporting Information, and for the unimolecular reactions in Figures 8 and 9.

An unexpected observation from the temperature-dependence experiments on the bimolecular reactions is that the slowest reacting of the *p*-substituted aniline radical cations for which measurements were made, $1\mathbf{b}^+$, has the smallest Arrhenius activation energy (Table 5). The other anilines have similar activation energies, within experimental error, and the difference in room temperature rates seems to be reflected more in the apparent Arrhenius preexponential factors ($\log(A)$, Table

TABLE 5. Kinetic Parameters for Deprotonation of Aniline Radical Cations with Tetrabutylammonium Acetate as the Base, in Acetonitrile Containing 0.5 M Water (0.9%) and 0.5 M Tetrabutylammonium Perchlorate

compd	$k_{-H^+}^a$ ($\text{M}^{-1} \text{ s}^{-1}$)	E_a^b (kcal/mol)	$\log(A)^b$ (s^{-1})
1b	4.1×10^7 (2.3×10^7) ^c	5.4 (6.6) ^c	11.8 (12.5) ^c
1c	1.2×10^8	7.0	13.3
1d	1.7×10^8	7.6	13.9
1e	1.4×10^9	6.6	14.0
4	3.6×10^9 (1.9×10^9) ^c	4.4 (4.3) ^c	12.7 (12.7) ^c

^a Bimolecular rate constant for deprotonation at room temperature. ^b Arrhenius activation energy, E_a , and intercept of Arrhenius plot, $\log(A)$. ^c Measured in acetonitrile/propionitrile solvent mixtures to simulate constant solvent polarity as a function of temperature; see Experimental Section.

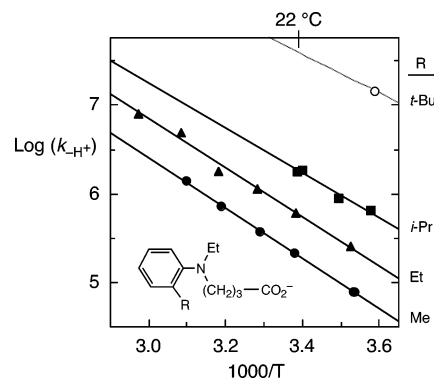


FIGURE 8. Plots of the logarithm of the rate constants for unimolecular deprotonation ($\log(k_{-H^+})$) versus reciprocal temperature, in acetonitrile with 20% water, for the ortho-substituted radical cations of the aniline derivatives $7\mathbf{b} - \mathbf{7e}$.

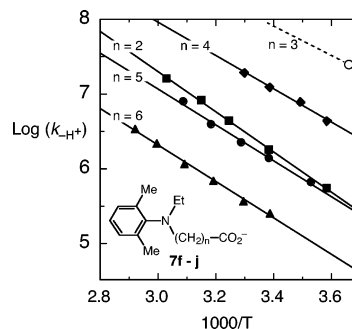


FIGURE 9. Plots the logarithm of the rate constants for unimolecular deprotonation ($\log(k_{-H^+})$) versus reciprocal temperature, in acetonitrile with 20% water, for the radical cations of the aniline derivatives $7\mathbf{f} - \mathbf{j}$.

5), which also seem to be larger than usually observed for bimolecular reactions in solution.²⁴

In related work on decarboxylation reactions of aniline radical cations, we observed unusual Arrhenius parameters due to temperature-dependent changes in solvation of the carboxylate.^{6b} The basicity of the acetate anion is expected to depend strongly upon solvent polarity. For example, the $\text{p}K_a$ of acetic acid increases dramatically upon going from water to acetonitrile.²⁵ We thus at-

(23) (a) Kirby, A. J. *Adv. Phys. Org. Chem.* **1980**, *17*, 183. (b) Mandolini, L. *Adv. Phys. Org. Chem.* **1986**, *22*, 1.

(24) Moore, J. W.; Pearson, R. G. *Kinetics and Mechanism*, 3rd ed.; Wiley: New York, 1981.

tempted to measure the kinetics of the reactions at different temperatures, but at constant polarity. The dielectric constant of most solvents decrease with increasing temperature.²⁶ Thus, mixtures of acetonitrile and propionitrile with 0.5 M water were prepared to obtain solutions that compensated for changes in solvent polarity with temperature, according to measurements with Reichardt's dye (see the Experimental Section for details). However, the data given in Table 5 indicate very little change in the Arrhenius parameters compared to experiments using only acetonitrile with 0.5 M water. This may be because specific hydration of the carboxylate with water dominates the solvation effects in all of the solvent mixtures used. Because of possible temperature-dependent carboxylate hydration, we have not attempted a detailed analysis of the Arrhenius data using, for example, transition state theory.

One general point can be made, however. In previous work on the radical cations of para-substituted *N,N*-dimethylaniline radical cations, Parker and Tilset reported extremely large activation entropies for deprotonation using acetate as the base, with values for ΔS^\ddagger of 35–53 eu.^{13b} The unusual activation entropies were interpreted in terms of a preequilibrium between the radical cation and the base.^{13b} Eyring analysis of the data in Table 5 (not shown) yields activation entropies that are all within 3 entropy units of zero, which is much closer to expected values for bimolecular reactions,²⁴ and suggests that there is no need to invoke a complex between the acid and the base, at least under the present conditions.

Even though we have not made a detailed analysis of the temperature-dependence data for the intramolecular reactions, we can see some clear empirical trends. For the ortho-substituted anilines, the intercepts of the Arrhenius plots (indicated as $\log(A)$ in the tables) are observed to be essentially the same within experimental error, i.e., ca. 15.²⁷ The differences in the rate constants at room temperature for these anilines are thus *empirically* due to differences in the slopes of the Arrhenius plots, Table 2. Deprotonation in the *o*-*tert*-butyl compound **7e** was too fast to measure at room temperature under the experimental conditions, and in fact could only be measured at one temperature, corresponding to the single point for this compound in Figure 8. If we assume that the temperature dependence for this reaction is the same as for **7b–d**, as indicated in Figure 8, then we can estimate a rate constant at room temperature of ca. $4 \times 10^7 \text{ s}^{-1}$, Table 2.

Corresponding temperature-dependent data for several of the compounds with varying methylene chain length are shown in Figure 9. Compared to the compounds in Figure 8, which all have a six-membered transition state, these reactions have different sized cyclic transition states, which may explain the larger differences in the intercepts of the Arrhenius plots in these cases. The deprotonation rate constant for the most reactive com-

pound, **7f**, was too high to measure at room temperature; however, a value was obtained at 0 °C (the single point in Figure 9). Assuming that the temperature dependence of this reaction is the same as for **7g–j**, as indicated in Figure 9, then we can estimate a rate constant of ca. $9 \times 10^7 \text{ s}^{-1}$ at room temperature, Table 3.

Determination of the absolute energetics of the proton-transfer reactions would require knowledge of the $\text{p}K_{\text{a}}$ of the acetate anion and the aniline radical cations under the experimental conditions. As mentioned above, the $\text{p}K_{\text{a}}$ of acetic acid increases dramatically from 4.75 in water to 22.3 in acetonitrile as a consequence of hydrogen bonding by water.²⁵ The corresponding increase in $\text{p}K_{\text{a}}$ of the radical cation of dimethylaniline is much smaller, i.e. from 11.4 to 19.4.²⁸ Thus, proton transfer from the *N,N*-dimethylaniline radical cation to acetate is endothermic in water by ca. 7 $\text{p}K_{\text{a}}$ units, and exothermic in acetonitrile by ca. 3 $\text{p}K_{\text{a}}$ units. However, the exothermicities of the reactions under the present conditions are difficult to determine, since the extent to which specific hydration reduces the basicity of the anionic acetate with 0.5 M water is not known.

As an illustration of the influence of water on the basicity of the acetate anion, the rate constant for deprotonation of the *p*-trifluoromethyl-*N,N*-dimethylaniline radical cation, **1e**, by acetate was measured in acetonitrile as a function of added water.²⁹ The bimolecular rate constant was ca. $6 \times 10^9 \text{ M}^{-1} \text{ s}^{-1}$ with no added water and decreased to $1.4 \times 10^9 \text{ M}^{-1} \text{ s}^{-1}$ at 0.9% water (0.5 M, see Table 1). The rate constant continues to decrease with increasing water concentration, becoming weakly dependent above ca. 4% water (2.2 M water), where the rate constant is ca. $10^8 \text{ M}^{-1} \text{ s}^{-1}$.²⁹ Similar observations were made by Mariano et al.^{8a} The rate constant with 0.5 M water is ca. 1 order of magnitude smaller than the diffusion-controlled limit, suggesting that this reaction *may* be close to thermoneutral, although it is not possible to say this with any certainty.

III. Summary

Deprotonation of aniline radical cations with an external base is typically slower than other fragmentation reactions of aniline radical cations under normal conditions, and is thus often less useful.^{8a} Reactivity toward deprotonation in *N,N*-dimethylanilines can be increased by the use of ortho substituents, which twist the non-bonding electrons on nitrogen out of conjugation with the ring. Based on this stereoelectronic effect, a series of aniline radical cations that undergo rapid unimolecular (intramolecular) deprotonation have been designed with rate constants for fragmentation controllable over 4 orders of magnitude, up to a value of ca. 10^8 s^{-1} in aqueous acetonitrile at room temperature. Control over the rate constant for fragmentation is important in the two-electron sensitization application of amine radical cations. The use of the intramolecular deprotonating

(25) Izutzu, K. *Acid-Base Dissociation Constants in Dipolar Aprotic Solvents*; Blackwell Scientific: Oxford, UK, 1990.

(26) Smyth, C. P. *Dielectric behavior and structure; dielectric constant and loss, dipole moment and molecular structure*; McGraw-Hill: New York, 1955.

(27) The meanings of the empirical E_{a} and $\log(A)$ values are clearly questionable if the basicity of the carboxylate is significantly temperature dependent.

(28) (a) Based on the thermodynamic calculations, the $\text{p}K_{\text{a}}$ differences in water and acetonitrile are principally due to differences in the free energies of solvation and the standard oxidation potentials of the hydrogen atom in the two solvents.^{28b} (b) Wayner, D. D. M.; Parker, V. D. *Acc. Chem. Res.* **1993**, *26*, 287.

(29) See Figure S4 in the Supporting Information.

anilines described here as two-electron sensitizers in silver halide photographic systems is described elsewhere.³⁰

IV. Experimental Section

Acetonitrile was spectrograde and used as received. Most of the para-substituted *N,N*-dimethylanilines were available from a previous study.¹⁵ *N,N*-Dimethyl-*o*-toluidine was obtained commercially and was distilled before use. *N,N*-Dimethyl-*p*-anisidine was prepared according to a literature procedure.³¹ The *N,N*-bis(trideuteriomethyl)anilines were prepared by either methylation of the corresponding anilines with CD₃I or reductive alkylation.³² Tetra-*n*-butylammonium acetate and tetra-*n*-butylammonium perchlorate were also obtained commercially. The acetate was recrystallized from dry ethyl acetate, dried in vacuo, and dispensed in a glovebox. The perchlorate was used as received. 9,10-Dicyananthracene, 9-cyanoanthracene, biphenyl, and 1,4-dimethoxybenzene were available from previous experimental work.¹⁷ The anilines with covalently attached carboxylates were prepared as described in the Supporting Information. Purity was checked with proton NMR spectroscopy.

The radical cations were generated with a time-resolved absorption apparatus and method that has been described in detail elsewhere,¹⁶ using either 9-cyanoanthracene (9-CA) or 9,10-dicyanoanthracene (DCA) as the sensitizers, with either 1,2-dimethoxybenzene or biphenyl as cosensitizers, respectively.¹⁶ In one case, *o*-*tert*-butyl-*N,N*-dimethylaniline, **3**, the *N*-methylquinolinium (NMQ)/toluene cosensitization system was used, to ensure rapid and irreversible oxidation of this sterically hindered molecule.³³ All of the anilines used in this work have lower oxidation potentials than that of the cosensitizers ($E^{\text{ox}} = 1.45$ V vs SCE for 1,2-dimethoxybenzene, $E^{\text{ox}} = 1.96$ V vs SCE for biphenyl, and $E^{\text{ox}} \leq 2.3$ V vs SCE for toluene),^{16,34} thus electron transfer from the aniline to the cosensitizer radical cation is energetically favorable and occurs with a rate constant that is essentially diffusion controlled. In all cases, the solutions were purged with oxygen. Oxygen oxidizes the 9-CA and DCA radical anions and NMQ radical by one-electron transfer to form the superoxide anion within ca. 100 ns under the conditions of the experiments, which would otherwise interfere with the absorptions of the radical cations.^{6,34a}

Experiments in which the rate constant for deprotonation of the radical cation **1c**⁺ was measured at varying concentrations of tetrabutylammonium perchlorate demonstrated that at first the rate of the reaction decreases rapidly with increasing salt concentration, but then becomes essentially independent of salt concentration above 0.4 and 0.6 M (data provided as Supporting Information, Figures S1 and S2).³⁵ Since the concentration of the acetate was ≤ 0.1 M in all of the experi-

ments, no change in the measured rate due to variation in ionic strength is expected.

The temperature dependencies of the rate constant for deprotonation of the radical cations of *p*-methyl-*N,N*-dimethylaniline, **1b**, and 2,6-dimethyl-*N,N*-dimethylaniline, **4**, were determined both with 0.5 M water in acetonitrile and in solvent mixtures that were designed to keep the polarity as constant with temperature as possible. These latter experiments were performed at 5, 25, 45, and 65 °C. The dielectric constants of propionitrile at 5 °C and acetonitrile at 65 °C are essentially identical, ca. 31–32.³⁶ The absorption maximum of Reichardt's dye³⁷ in acetonitrile with 0.5 M water at 65 °C is 592 nm, and in propionitrile with 0.5 M water at 5 °C it is 605 nm. Mixtures of acetonitrile and propionitrile with 0.5 M water at intermediate temperatures were determined empirically to give a solution of Reichardt's dye with absorption maxima between these two values. At 25 °C, the solvent mixture 60:40 propionitrile:acetonitrile with 0.5 M water gave an absorption maximum at 596 nm. At 45 °C, the solvent mixture 30:70 propionitrile:acetonitrile with 0.5 M water gave an absorption maximum at 602 nm. Determination of the rate constant for deprotonation at these four temperatures in these solvents gave the Arrhenius data shown in Table 5.

The errors in the rate constants and Arrhenius activation parameters are estimated to be less than 15%, based upon repeated measurements.

The oxidation potentials of the anilines were measured by using square-wave voltammetry, and details are as described in ref 16. Measurements were performed in dry acetonitrile with use of a 10 μm Pt working electrode. The reference potential was established with use of the ferrocene/ferrocenium couple. The oxidation potentials were then corrected to the SCE electrode by the addition of 0.4 V.

Electronic structure calculations were performed with the Spartan '02 software package (version 1.0.6),³⁸ and the optimizations were done by using the B3LYP DFT method with a 6-31G* basis set.

Acknowledgment. We thank the National Science Foundation for research support (CHE-9812719 and CHE-0213445) and Deniz Schildkraut (Eastman Kodak Company) for performing the electrochemical measurements.

Supporting Information Available: Synthetic details for compounds **7** and **8**, plots showing k_{obs} vs $[\text{Bu}_4\text{N}^+ \text{OAc}]$ at various $[\text{Bu}_4\text{N}^+ \text{ClO}_4]$ for **1c**⁺, the dependence of $k_{-\text{H}^+}$ as a function of $[\text{Bu}_4\text{N}^+ \text{ClO}_4]$ for **1c**⁺, the transient absorption spectrum of **3**⁺ as a function of time, the dependence of $k_{-\text{H}^+}$ for **1e**⁺ in acetonitrile on added water, Arrhenius plots for deprotonation of radical cations **1**⁺ by acetate in acetonitrile with 0.5 M water and 0.5 M tetrabutylammonium perchlorate, and Cartesian coordinates for the minimum geometries of radical cations **1**⁺–**5**⁺. This material is available free of charge via the Internet at <http://pubs.acs.org>.

JO047813G

(30) Gould, I. R.; Farid, S.; Godleski, S. A.; Lenhard, J. R.; Muentner, A. A.; Zielinski, P. A. U.S. Patent 5 994 051, Nov. 30, 1999.

(31) Davies, W. C. *Bull. Soc. Chim. Fr.* **1935**, 2, 295.

(32) Dinnocenzo, J. P.; Karki, S. B.; Jones, J. P. *J. Am. Chem. Soc.* **1993**, 115, 7111.

(33) Dockery, K. P.; Dinnocenzo, J. P.; Farid, S.; Goodman, J. L.; Gould, I. R.; Todd, W. P. *J. Am. Chem. Soc.* **1997**, 119, 1876.

(34) (a) Guirado, G.; Fleming, C. N.; Lingemfelter, T. G.; Williams, M. L.; Zuilhof, H.; Dinnocenzo, J. P. *J. Am. Chem. Soc.* **2004**, 126, 14086. (b) Zweig, A.; Hodgson, W. G.; Jura, W. H. *J. Am. Chem. Soc.* **1964**, 86, 4124.

(35) See also ref 8a.

(36) Wohlfarth, C. In *CRC Handbook of Chemistry and Physics*, 76th ed.; Lide, D. R., Ed.; CRC Press: Boca Raton, FL, 1995; p 6-193.

(37) Reichardt, C. *Solvents and Solvent Effects in Organic Chemistry*, 2nd ed.; VCH: Weinheim, Germany, 1988; pp 285–311.

(38) Wavefunction, Inc., Irvine, CA.